Geometrical Isomer Preference of Ru^{II} and Ru^{III}: Chemistry and Structure of a RuS_4P_2 Family. Crystal Structure of $[Ru(PhCH_2SCS_2)_2(PPh_3)_2]$†

Amitava Pramanik, Nilkamal Bag, Goutam Kumar Lahiri, and Animesh Chakravorty *
Department of Inorganic Chemistry, Indian Association for the Cultivation of Science, Calcutta 700032, India

The syntheses of mixed thioxanthate (trithiocarbonate)–phosphine complexes of types *cis*-$[Ru(RSCS_2)_2(PPh_3)_2]$ (**1**) and *trans*-$[Ru(RSCS_2)_2(PPh_3)_2]PF_6$ ($\mathbf{2}^+$) are reported (R = Et, Pr^i, or $PhCH_2$). These along with *trans*-$[Ru(RSCS_2)_2(PPh_3)_2]$ (**2**) and *cis*-$[Ru(RSCS_2)_2(PPh_3)_2]^+$ ($\mathbf{1}^+$) constitute an electrochemically observable redox isomerisation cycle. The formal potentials of the couples ($\mathbf{1}^+$)–(**1**) and ($\mathbf{2}^+$)–(**2**) are ≈0.65 and ≈0.33 V respectively *vs.* saturated calomel electrode (s.c.e.). The isomerisation steps are ($\mathbf{1}^+$) ⟶ ($\mathbf{2}^+$) (fast) and (**2**) ⟶ (**1**) ($k \approx 7.0 \times 10^{-2}$ s^{-1}). The *X*-ray structure of complex (**1**; R = $PhCH_2$) has been determined: space group *C*2/*c*, *a* = 18.676(7), *b* = 10.511(2), *c* = 24.432(8) Å, and *Z* = 4. The superior stability of the *cis* configuration of Ru^{II} for complexes (**1**) arises primarily from the strong back-bonding (*cis* > *trans*) within the $Ru(PPh_3)_2$ fragment. For Ru^{III}, in which back-bonding is unimportant, the stable geometry is *trans* owing to favourable steric disposition of the PPh_3 molecules. The frozen glass e.s.r. spectra of complexes ($\mathbf{2}^+$) have a sizable axial distortion ($\Delta \approx 8\,500$ cm^{-1}) with a relatively small rhombic component ($V \approx 2\,200$ cm^{-1}). One of the two predicted transitions ($\nu_1 \approx 7\,500$ and $\nu_2 \approx 9\,900$ cm^{-1}) within the t_{2g} shell is observable ($\nu_1 \approx 6\,500$ cm^{-1}) in the near-i.r. region.

This work stems from our interest in geometrical isomerisation of metal complexes promoted by metal redox.[1] We have been in search of systems where the structural origin of this phenomenon is experimentally tractable. In this context we have synthesised and characterised a hitherto unknown family of ruthenium thioxanthates (trithiocarbonates) containing triphenylphosphine, $[Ru(RSCS_2)_2(PPh_3)_2]^z$ ($z = 0$ or $+1$), in which the RuS_4P_2 co-ordination sphere is geometrically responsive to metal redox. The stable forms are *cis*-$Ru^{II}S_4P_2$ and *trans*-$Ru^{III}S_4P_2$. The forms *trans*-$Ru^{II}S_4P_2$ and *cis*-$Ru^{III}S_4P_2$ are accessible *via* rapid redox but the mismatch between geometry and oxidation state is corrected by spontaneous isomerisation. The *X*-ray structure of *cis*-$[Ru^{II}(PhCH_2SCS_2)_2(PPh_3)_2]$ has been determined. This has partly clarified the role of back-bonding and steric interaction within the $Ru(PPh_3)_2$ fragment in isomer differentiation by metal oxidation states.

Results and Discussion

Synthesis.—The four types of $[Ru(RSCS_2)_2(PPh_3)_2]^z$ ($z = 0$ or $+1$) species studied are *cis*-Ru^{II} (**1**), *cis*-Ru^{III} ($\mathbf{1}^+$), *trans*-Ru^{II} (**2**), and *trans*-Ru^{III} ($\mathbf{2}^+$). Among these (**1**) and ($\mathbf{2}^+$) have been isolated in the pure state. Complexes (**2**) are electrochemically observable in cold solutions but ($\mathbf{1}^+$) remain elusive due to very rapid isomerisation (see below). The only thioxanthate of ruthenium reported previously appears to be $[Ru(MeSCS_2)_2(CO)_2]$.[2]

The reaction between $[Ru(PPh_3)_3Cl_2]$ and $Na(S_2CSR)$ in refluxing ethanol proceeds as in equation (1) and affords

$$[Ru(PPh_3)_3Cl_2] + 2Na(S_2CSR) \longrightarrow \mathbf{(1)} + PPh_3 + 2NaCl \quad (1)$$

complexes (**1**) in quantitative yields as orange-yellow crystals. Oxidation of complexes (**1**) in dichloromethane–acetonitrile by aqueous cerium(IV) [equation (2)] forms the red-brown

$$\mathbf{(1)} + Ce^{IV} + PF_6^- \longrightarrow \mathbf{(2)}^+PF_6^- + Ce^{III} \quad (2)$$

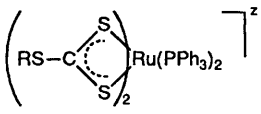

R = Et, Pr^i, or $PhCH_2$

(**1**) *cis*, *z* = 0
($\mathbf{1}^+$) *cis*, *z* = +1
(**2**) *trans*, *z* = 0
($\mathbf{2}^+$) *trans*, *z* = +1

complexes ($\mathbf{2}^+$) quantitatively *via* rapid isomerisation of ($\mathbf{1}^+$) formed initially. Complexes ($\mathbf{2}^+$), isolated as their PF_6^- salts, behave as 1:1 electrolytes in acetonitrile (Λ = 140—150 Ω^{-1} cm^2 mol^{-1}). Analytical and electronic spectral data for (**1**) and ($\mathbf{2}^+$) are collected in Table 1 and representative electronic spectra are displayed in Figure 1.

X-*Ray Crystal Structure of cis*-$[Ru(PhCH_2SCS_2)_2(PPh_3)_2]$.—The lattice consists of discrete molecules each having a crystallographically imposed two-fold axis of symmetry. A view of the molecule is shown in Figure 2 and selected bond distances and angles are listed in Table 2. The four-membered chelate ring is grossly planar (mean deviation 0.038 Å), with a small fold (7.3°) along the S(1)S(2) axis. The RuS_4P_2 co-ordination sphere (C_2 point group) displays large angular deviations from idealised octahedral geometry.

The steric interaction between the two *cis* phosphine ligands is reflected in the structural data. The three carbon atoms directly bonded to P(1) are staggered (when viewed along the PP axis)[3] with respect to those similarly bonded to P(1a) (see

† *cis*-Bis(benzyl trithiocarbonato-*S*,*S*′)bis(triphenylphosphine)-ruthenium(II).

Supplementary data available: see Instructions for Authors, *J. Chem. Soc., Dalton Trans.*, 1990, Issue 1, pp. xix—xxii.

Table 1. Analytical[a] and electronic spectral data[b]

Compound	Elemental analysis (%) C	H	U.v.–visible and near-i.r. spectral data, $\lambda_{max.}$/nm (ε/dm^3 mol^{-1} cm^{-1})
cis-[Ru(EtSCS$_2$)$_2$(PPh$_3$)$_2$]	56.15 (56.05)	4.50 (4.45)	415 (7 270), 325 (9 290), 260 (36 400)
cis-[Ru(Pr^{i}SCS$_2$)$_2$(PPh$_3$)$_2$]	56.90 (56.95)	4.80 (4.75)	415 (5 170), 325 (6 960), 255 (32 600)
cis-[Ru(PhCH$_2$SCS$_2$)$_2$(PPh$_3$)$_2$]	61.10 (61.00)	4.25 (4.30)	425 (7 280), 325 (8 980), 265 (35 800)
trans-[Ru(EtSCS$_2$)$_2$(PPh$_3$)$_2$]PF$_6$	48.35 (48.25)	3.75 (3.85)	1 550 (36), 760 (3 430), 420 (11 280), 295 (34 000)
trans-[Ru(Pr^{i}SCS$_2$)$_2$(PPh$_3$)$_2$]PF$_6$	49.30 (49.25)	4.20 (4.10)	1 550 (30), 760 (3 070), 415 (9 240), 290 (30 900)
trans-[Ru(PhCH$_2$SCS$_2$)$_2$(PPh$_3$)$_2$]PF$_6$	53.40 (53.40)	3.80 (3.75)	1 500 (35), 760 (3 220), 425 (12 540), 295 (35 800)

[a] Calculated values are in parentheses. [b] In dichloromethane at 298 K.

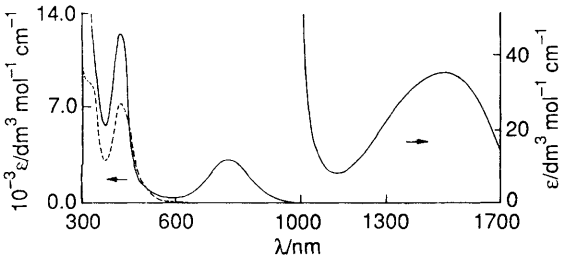

Figure 1. Electronic spectra of *cis*-[Ru(PhCH$_2$SCS$_2$)$_2$(PPh$_3$)$_2$] (– – – –) and *trans*-[Ru(PhCH$_2$SCS$_2$)$_2$(PPh$_3$)$_2$]PF$_6$ (——) in dichloromethane at 298 K

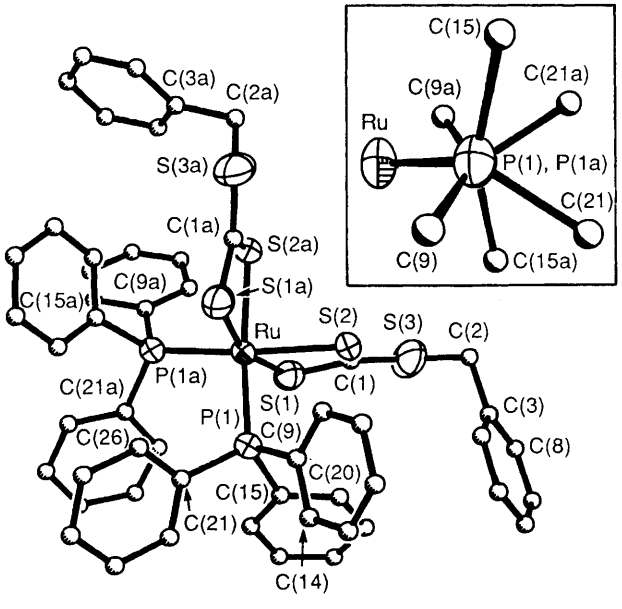

Figure 2. An ORTEP plot for *cis*-[Ru(PhCH$_2$SCS$_2$)$_2$(PPh$_3$)$_2$]

inset in Figure 2). The P(1)–Ru–P(1a) angle of 102.0(1)° is expanded significantly from octahedral. The observed stability of the *cis* configuration implies the presence of strong electronic factors which more than offset the steric disadvantage.

The two Ru–S distances are unequal; the longer and shorter distances, 2.436(1) and 2.400(2) Å, respectively correspond to sulphur atoms *trans* and *cis* to phosphorus atoms. The distances

Table 2. Selected bond lengths (Å) and angles (°) for *cis*-[Ru(PhCH$_2$SCS$_2$)$_2$(PPh$_3$)$_2$]

Ru–P(1)	2.326(1)	C(1)–S(1)	1.676(5)
Ru–S(1)	2.400(2)	C(1)–S(2)	1.694(5)
Ru–S(2)	2.436(1)	C(1)–S(3)	1.730(5)
P(1)–Ru–S(1)	95.4(1)	S(1)–Ru–S(2a)	94.7(1)
P(1)–Ru–S(2)	87.6(1)	S(2)–Ru–S(2a)	85.4(1)
P(1)–Ru–P(1a)	102.0(1)	Ru–S(1)–C(1)	88.4(2)
P(1)–Ru–S(1a)	96.4(1)	Ru–S(2)–C(1)	86.8(2)
P(1)–Ru–S(2a)	165.1(1)	S(1)–C(1)–S(2)	113.2(3)
S(1)–Ru–S(2)	71.1(1)	S(1)–C(1)–S(3)	121.1(3)
S(1)–Ru–S(1a)	161.2(1)	S(2)–C(1)–S(3)	125.7(3)

within the thioxanthate ligand agree with those in other structurally characterised thioxanthate complexes[4] including osmium species.[5]

E.S.R. Spectra of trans-[Ru(RSCS$_2$)$_2$(PPh$_3$)$_2$]PF$_6$.—*X*-Ray-quality single crystals of this category of compounds could not be grown. However, e.s.r. and electrochemical (see below) results taken collectively are in agreement for a *trans* geometry. The magnetic moments of complexes (**2**$^+$) correspond to one unpaired electron (Table 3). E.s.r. spectra measured in frozen glass (dichloromethane–toluene, 77 K) are rhombic in nature but with closely spaced g_x and g_y signals (Figure 3). The g values were used to quantitate both the axial distortion (Δ) which splits the t_2 shell into $e + b$ levels and the rhombic distortion (V) which splits e further into two non-degenerate compounds.[6] Taking λ the spin-orbit coupling for Ru^{III} as 1 000 cm^{-1},[7] two ligand-field transitions are predicted within the Kramers doublets at ≈7 500 (ν_1) and ~9 900 cm^{-1} (ν_2). One of these (ν_1) is experimentally observable at ≈6 500 cm^{-1} (Table 3, Figure 1) but owing to a rapid rise in absorption pertaining to nearby intense transitions the ν_2 band is not seen.

The g_x and g_y signals can be considered to represent split components of $g_{\|}$ for the idealised tetragonal *trans*-RuS$_4$P$_2$ co-ordination sphere. The chelate rings and the phosphine phenyls are expected to provide only a relatively small rhombic perturbation as is observed in practice.

Metal Redox and Isomerisation.—Voltammetric redox experiments were performed in the temperature range 248—300 K in dichloromethane solution at a platinum working electrode. Representative results are displayed in Figure 4 and these can be rationalised in terms of isomerisation following metal redox. The behaviour of complexes (**1**) is considered first

Table 3. Magnetic moments,[a] assignments of e.s.r. g values,[b] distortion parameters, and near-i.r. transitions[c] for *trans*-$[Ru(RSCS_2)_2(PPh_3)_2]PF_6$

R	$\mu_{eff.}$	g_x	g_y	g_z	Δ/λ	V/λ	ν_1/λ	ν_2/λ	ν_1/λ Obs.[d]
Et	1.87	−2.401	−2.303	1.946	8.586	−2.248	7.465	9.894	6.450
Pr^i	1.95	−2.403	−2.306	1.943	8.326	−2.281	7.194	9.651	6.450
$PhCH_2$	1.90	−2.398	−2.309	1.948	8.763	−2.085	7.714	9.995	6.670

[a] In the solid state at 298 K. [b] Measurements were made in dichloromethane–toluene (1:1) glass at 77 K. [c] Symbols have the same meaning as in the text. [d] Observed frequency converted to ν_1/λ by setting $\lambda = 1\,000\ cm^{-1}$.

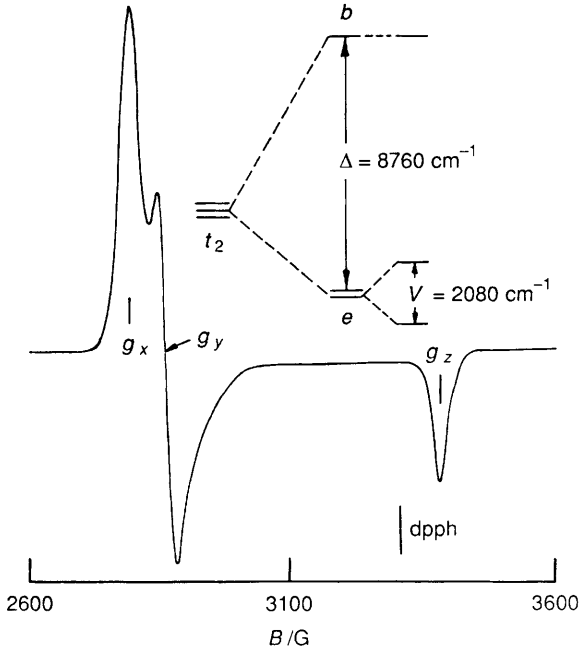

Figure 3. *X*-Band e.s.r. spectrum and t_2 splittings of *trans*-$[Ru(PhCH_2SCS_2)_2(PPh_3)_2]PF_6$ in dichloromethane–toluene (1:1) glass (77 K); dpph = diphenylpicrylhydrazyl

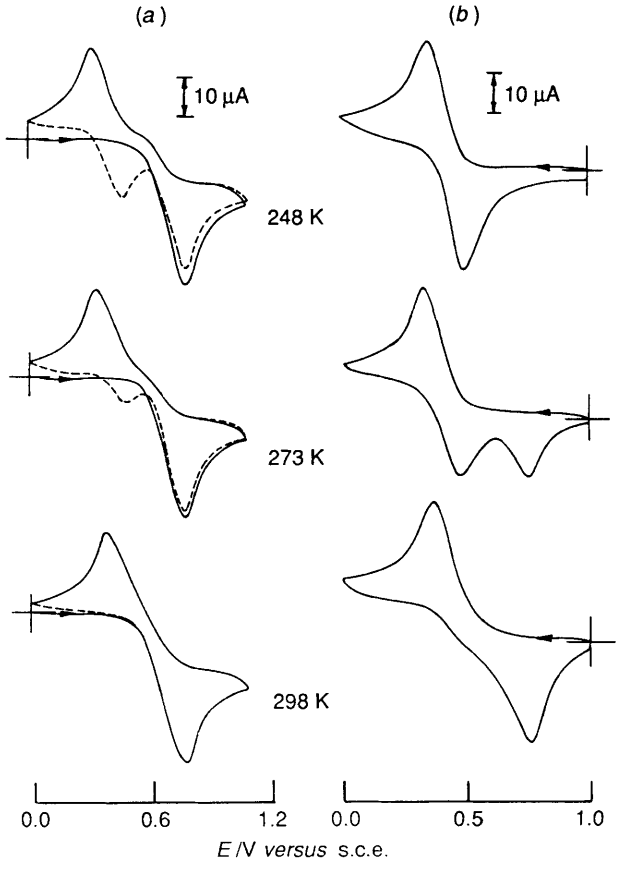

Figure 4. Variable-temperature cyclic voltammograms (scan rate 50 mV s^{-1}) of $\approx 10^{-3}$ mol dm^{-3} solutions of (*a*) *cis*-$[Ru(PhCH_2SCS_2)_2(PPh_3)_2]$ [first cycle (——), second cycle (– – – –)] and (*b*) *trans*-$[Ru(PhCH_2SCS_2)_2(PPh_3)_2]PF_6$ in dichloromethane (0.1 mol dm^{-3} $[NEt_4][ClO_4]$) at a platinum electrode

[Figure 4(*a*)]. At 298 K the voltammogram shows an anodic peak due to stereoretentive one-electron (confirmed coulometrically) oxidation to (1^+). Electrogenerated (1^+) isomerises rapidly to (2^+) and the cathodic peak due to the reduction of (1^+) is not observed on scan reversal. Instead the reduction of (2^+) is seen at a potential $\approx$400 mV lower than the the anodic peak of (**1**). The same voltammogram is obtained in the second and subsequent cycles indicating that the isomerisation processes $(1^+) \longrightarrow (2^+)$ and $(2) \longrightarrow (1)$ are both fast at 298 K. Upon cooling the solution, the first cyclic voltammogram remains unchanged but in later cycles both the anodic and cathodic responses arising from the *trans* isomer are observable as a result of the retarded isomerisation $(2) \longrightarrow (1)$. The isomerisation $(1^+) \longrightarrow (2^+)$ however remains fast throughout the temperature range studied and the cathodic peak due to (1^+) could not be observed even by use of a high scan rate (1 V s^{-1}) at 248 K. The processes considered above are stated in equations (**3**)—(**6**).

$$(1^+) + e \rightleftharpoons (1) \quad (3)$$

$$(1^+) \xrightarrow{fast} (2^+) \quad (4)$$

$$(2^+) + e \rightleftharpoons (2) \quad (5)$$

$$(2) \xrightarrow{k} (1) \quad (6)$$

The voltammograms arising from pure (2^+) [Figure 4(*b*)] are entirely in agreement with the above. Here the uncomplicated one-electron process involving (2^+) and (**2**) [equation (5)] is observable at 248 K. Upon raising the temperature, isomerisation of electrogenerated (**2**) into (**1**) occurs and finally at 298 K the voltammogram matches that of (**1**).

Cyclic voltammetric current height data of (2^+) was used to compute[8] the first-order rate constants k of the *trans*-to-*cis* isomerisation reaction of equation (6). Variable-temperature data afforded the activation parameters listed in Table 4. The large, negative entropy factor is in agreement with the occurrence of a twist pathway.[9]

The formal potentials $E°(cis)$ and $E°(trans)$ of the couples of equations (3) and (5) respectively are listed in Table 5, the *cis* potentials being systematically higher than the *trans* potentials, $E°(cis) > E°(trans)$. The equilibrium constant (K^{cr}) of the cross

Table 4. Rate constants and activation parameters in dichloromethane for bivalent *trans* ⟶ *cis* isomerisation

R	T/K	k/s^{-1}	$\Delta H^{\ddagger}$/ kJ mol^{-1}	$\Delta S^{\ddagger}$/ J K^{-1} mol^{-1}
Et	268	5.3×10^{-2}	55.3	−65.2
	273	7.5×10^{-2}		
	278	13.3×10^{-2}		
Pr^{i}	268	3.0×10^{-2}	54.3	−73.5
	273	4.6×10^{-2}		
	278	7.4×10^{-2}		
$PhCH_2$	268	4.2×10^{-2}	48.7	−91.8
	273	5.9×10^{-2}		
	278	9.3×10^{-2}		

Table 5. Electrochemical data[a]

R	Ru^{III}–Ru^{II} couples, E_{248}°/V *cis*[b]	*trans*	$10^{-6}K^{cr}$[c]
Et	0.61	0.29	3.16
Pr^{i}	0.64	0.32	3.16
$PhCH_2$	0.71	0.38	5.05

[a] Conditions: solvent, dichloromethane; supporting electrolyte, NEt_4ClO_4 (0.1 mol dm^{-3}); working electrode, platinum; reference electrode, saturated calomel electrode (s.c.e.); solute concentration, $\approx 10^{-3}$ mol dm^{-3}. Cyclic voltammetric data: $E_{248}° = 0.5\ (E_{p_a} + E_{p_c})$, where E_{p_a} and E_{p_c} are anodic and cathodic peak potentials respectively at 248 K; scan rate, 50 mV s^{-1}. [b] For the *cis* isomer E_{p_c} is not observed; $E_{248}°$ is calculated by assuming that peak-to-peak separation is 150 mV which is the observed average separation of E_{p_a} and E_{p_c} in *trans* isomers. [c] From equation (8).

reaction (at 248 K) [equation (7)] is related to $E°(cis)$ and

$$(2) + (1^+) \rightleftharpoons (1) + (2^+) \qquad (7)$$

$E°(trans)$ by equation (8). Computed K^{cr} values are given in

$$K^{cr} = \exp\{46.77[E°(cis) - E°(trans)]\} \qquad (8)$$

Table 5. The large ($\approx 10^6$) K^{cr} values reflect the high stability of (**1**) and (**2**$^+$) compared to (**2**) and (**1**$^+$).

Origin of Isomer Differentiation.—The structural results throw light on the origin of isomer differentiation. The remarkable stability of the *cis* geometry in spite of phosphine–phosphine steric hindrance is logically attributed to strong $4d\pi$–$3d\pi$ back-bonding in the $Ru^{II}P_2$ fragment. Back-bonding is expected to be stronger in the *cis* than in the *trans* form, all three ruthenium $4d\pi$ orbitals being suitable for π-bonding only in the former: hence the superior stability of (**1**) over (**2**). This explanation is also consistent with the trend of reduction potentials, $E°(cis) > E°(trans)$. The redox electron in the couples (**1**$^+$)–(**1**) and (**2**$^+$)–(**2**) is located in the $4d\pi$ orbital, stronger back-bonding providing greater stability for this orbital in the *cis* form.

Ruthenium(III) is a poor π-donor[10] and back-bonding may be expected to be very weak or totally absent in $[Ru(RSCS_2)_2(PPh_3)_2]^+$. The phosphine–phosphine steric interaction (*trans* ≪ *cis*) is then expected to become controlling and this explains the stability order (**2**$^+$) ≫ (**1**$^+$). Thus isomerisation occurs to maximise back-bonding when it is of significance (bivalent, *trans* ⟶ *cis*) or to relieve steric crowding where back-bonding is weak (trivalent, *cis* ⟶ *trans*).

Earlier we reported[11] the metal redox and isomerisation of ruthenium xanthates of type $[Ru(ROCS_2)_2(PPh_3)_2]^z$ ($z = 0$ or $+1$). The gross features are similar to those reported here. Unfortunately the lack of single crystals precluded a structure determination for this system. In view of the present results it is very likely that the isomer preference in $[Ru(ROCS_2)_2(PPh_3)_2]^z$ is also controlled by similar electronic and steric factors operating primarily within the RuP_2 fragment. Structural and reactivity studies in progress on the osmium analogues $[Os(ROCS_2)_2(PPh_3)_2]^z$ and $[Os(RSCS_2)_2(PPh_3)_2]^z$ are consistent[5] with the proposals made above.

Conclusion

In the $[Ru(RSCS_2)_2(PPh_3)_2]^z$ ($z = 0$ or $+1$) family the stable co-ordination spheres are *cis*-$Ru^{II}S_4P_2$ and *trans*-$Ru^{III}S_4P_2$. Stability is controlled by a balance of electronic and steric factors primarily within the $Ru(PPh_3)_2$ fragment. The inequality $E°(cis) > E°(trans)$ derives from the superior back-bonding in *cis*- compared to *trans*-$Ru^{II}S_4P_2$. Redox-driven isomerisation reactions are known among metal carbonyl species but in no case has it been possible to probe the origin in terms of experimental bond parameters.[12–14] Among non-carbonyl species very few examples of redox promoted isomerisation have been documented.[1,5,15] Systematic investigations will no doubt reveal many more examples and will clarify the factors that control this phenomenon in different situations. We are currently trying to define and rationalise the effect of the systematic variation of donor atoms on redox-driven isomerisation in complexes of type RuA_4B_2.

Experimental

Materials.—Commercial ruthenium trichloride was received from Arora Matthey, Calcutta, India and purified by repeated evaporation to dryness with concentrated hydrochloric acid.[16] The compound $[Ru(PPh_3)_3Cl_2]$ was prepared according to the reported procedure.[17] Preparation of $Na(S_2CSR)$ salts were as reported.[4a] The preparation of tetraethylammonium perchlorate and the purification of dichloromethane and acetonitrile for electrochemical/spectroscopic work were done as before.[1] All other chemicals and solvents were of reagent grade and used without further purification.

Physical Measurements.—U.v.–visible and near-i.r. spectra were recorded by using a Hitachi 330 spectrophotometer, i.r. (4 000—300 cm^{-1}) spectra on a Perkin-Elmer 783 spectrophotometer. Magnetic susceptibilities were measured on a PAR 155 vibrating-sample magnetometer. Electrochemical, e.s.r., and microanalytical measurements were done as before.[1] Low-temperature electrochemical measurements were done with the help of a Haake model F3-K digital cryostat and circulator connected with jacketed cell bottoms. Solution electrical conductivity was measured by using a Philips PR 9500 bridge.

Preparation of Complexes.—The syntheses of complexes were achieved by using general procedures. Yields varied in the range 90—95%. Details are given only for one representative complex of each type.

cis-*Bis(benzyl trithiocarbonato)bis(triphenylphosphine)-ruthenium*(II), *cis*-$[Ru(PhCH_2SCS_2)_2(PPh_3)_2]$. To a warm solution of $[Ru(PPh_3)_3Cl_2]$ (100 mg, 0.10 mmol) in ethanol (30 cm^3) was added $Na(S_2CSCH_2Ph)$ (60 mg, 0.27 mmol). The mixture was refluxed for 1 h. Upon cooling an orange-yellow microcrystalline solid separated which was collected by filtration, washed thoroughly with water and ethanol, and dried *in vacuo* over P_4O_{10}. Yield 90%.

Table 6. Atomic co-ordinates ($\times 10^4$) for *cis*-[Ru($PhCH_2SCS_2$)$_2$(PPh_3)$_2$]

Atom	*x*	*y*	*z*
Ru	0	2 935(1)	2 500
P(1)	−65(1)	4 327(1)	1 753(1)
S(1)	1 281(1)	2 561(1)	2 586(1)
S(2)	206(1)	1 231(1)	1 868(1)
S(3)	1 775(1)	327(2)	2 006(1)
C(9)	−595(2)	3 775(4)	1 086(2)
C(15)	816(2)	4 647(4)	1 538(2)
C(10)	−1 033(3)	2 713(5)	1 040(2)
C(1)	1 097(3)	1 347(4)	2 141(2)
C(2)	1 376(5)	−577(5)	1 401(3)
C(14)	−568(3)	4 471(5)	606(2)
C(11)	−1 426(3)	2 354(6)	528(2)
C(12)	−1 392(4)	3 046(7)	62(2)
C(13)	−962(4)	4 091(7)	103(2)
C(20)	1 085(3)	3 758(4)	1 207(2)
C(19)	1 772(3)	3 863(6)	1 073(2)
C(3)	1 421(4)	93(6)	859(3)
C(18)	2 193(3)	4 880(7)	1 247(3)
C(7)	2 141(5)	787(8)	194(3)
C(4)	824(5)	632(8)	533(3)
C(8)	2 074(4)	177(7)	669(3)
C(16)	1 263(3)	5 649(6)	1 723(3)
C(17)	1 952(3)	5 751(7)	1 567(3)
C(6)	1 553(5)	1 341(9)	−118(3)
C(5)	896(5)	1 275(9)	58(3)
C(21)	−511(2)	5 878(4)	1 776(2)
C(22)[a]	−271(4)	6 937(8)	1 486(3)
C(23)[a]	−603(5)	8 159(9)	1 507(4)
C(24)[a]	−1 360(6)	8 021(12)	1 944(5)
C(25)[b]	−1 673(19)	7 045(32)	1 986(15)
C(26)[b]	−1 242(14)	5 895(25)	1 913(12)
C(22a)[a]	−159(6)	6 989(10)	2 065(5)
C(23a)[a]	−630(7)	8 082(12)	2 125(6)
C(26b)[b]	−1 234(8)	5 820(14)	1 673(6)
C(25b)[b]	−1 467(9)	7 253(16)	1 990(7)
C(26a)[b]	−1 108(12)	6 023(22)	2 007(10)
C(25a)[b]	−1 646(9)	6 924(14)	1 736(6)
C(24a)[a]	−1 166(6)	8 263(10)	1 770(4)

[a] Site occupation 0.500. [b] Site occupation 0.333.

trans-*Bis*(*benzyl trithiocarbonato*)*bis*(*triphenylphosphine*)-*ruthenium*(III) *hexafluorophosphate*, *trans*-[Ru($PhCH_2SCS_2$)$_2$(PPh_3)$_2$]PF_6. To a solution of pure *cis*-[Ru($PhCH_2SCS_2$)$_2$(PPh_3)$_2$] (100 mg, 0.10 mmol) in dichloromethane–acetonitrile (1:10, 30 cm^3) was added ceric ammonium sulphate (100 mg, 0.70 mmol) dissolved in water (25 cm^3). The mixture was stirred magnetically for 3 h during which the colour of the solution became red-brown. The reaction mixture was then filtered and the filtrate concentrated to 10 cm^3 under reduced pressure and a saturated aqueous solution of NH_4PF_6 (10 cm^3) added. The solid thus obtained was collected by filtration, washed with water, and dried *in vacuo* over P_4O_{10}. The crude product was dissolved in a small volume of dichloromethane and subjected to chromatography on a silica gel (60—120 mesh, BDH) column (30 × 1 cm). On elution with benzene–acetonitrile (9:1) a red-brown band moved out and was collected. The desired complex was obtained from the eluant in crystalline form by slow evaporation.

Treatment of E.S.R. Data.—The details of the method used for assigning the observed signals to g_x, g_y, and g_z have been given in recent publications.[6c–e] We note that a second solution also exists which differs from the chosen one, having small values of Δ, V, ν_1, and ν_2; however the near-i.r. results clearly eliminate this alternative solution.

Kinetic Measurements.—The *trans* ⟶ *cis* isomerisation (**2**) ⟶ (**1**) was followed electrochemically. The anodic current height due to the (2^+)–(**2**) couple was monitored as a function of the switching potential and the rate constants (k) at different temperatures computed according to an available procedure.[8] The activation parameters $\Delta H^{\ddagger}$ and $\Delta S^{\ddagger}$ were obtained from an Eyring plot.[18]

X-*Ray Structure Determination.*—*Crystal data.* Single crystals were grown by slow diffusion of hexane into a dichloromethane solution of (**1**, R = CH_2Ph). $C_{52}H_{44}P_2S_6Ru$, M = 1 024.2, monoclinic, space group $C2/c$, a = 18.676(7), b = 10.511(2), c = 24.432(8) Å, β = 99.42(3)°, U = 4 732(2) Å^3 (by least-squares refinement of diffractometer angles for 25 automatically centred reflections), Z = 4, D_c = 1.438 g cm^{-3}, orange parallelopiped (0.20 × 0.24 × 0.34 mm), μ(Mo-K_α) = 6.80 cm^{-1}, λ = 0.710 73 Å, F(000) = 2 104.

Data collection and processing. Nicolet R3m/V diffractometer, ω-scan method ($2 \leqslant 2\theta \leqslant 55°$), graphite-monochromated Mo-K_α radiation; 5 372 independent reflections, 3 424 observed reflections [$F > 6\sigma(F)$], corrected for Lorentz and polarisation factors; semiempirical absorption correction (transmission 0.7305—0.7683). Two standard reflections monitored showed no significant variations.

Solution and refinement. The structure was solved by using the heavy-atom method, the position of the metal atom being determined from a Patterson map and the remaining non-hydrogen atoms by successive Fourier-difference syntheses. The refinement was done by full-matrix least-squares procedures. One phenyl ring [C(21)—C(26)] is shown in a fixed condition (Figure 2) but was actually disordered. All non-hydrogen atoms (except disordered carbon atoms) were refined with anisotropic thermal parameters. Hydrogen atoms were included (except those for the disordered carbons) at calculated positions with isotropic thermal parameters (0.08 Å^2). The final residuals R and R' were 0.043 and 0.058 respectively. The function minimised was $\Sigma w(|F| - |F_c|)^2$ with weight, $w = 1/[\sigma^2(F) + 0.0007F^2]$. The maximum and minimum residual electron densities in the final ΔF map were 0.50 and −0.48 e Å^{-3} respectively. Positional parameters for the non-hydrogen atoms are collected in Table 6. Computations were carried out on a Micro VAX II computer using the SHELXTL-PLUS program system.[19] The diagram was drawn using ORTEP.[20]

Additional material available from the Cambridge Crystallographic Data Centre comprises H-atom co-ordinates, thermal parameters, and remaining bond lengths and angles.

Acknowledgements

We are very grateful to the Department of Science and Technology, New Delhi, for establishing a National Single Diffractometer Facility at the Department of Inorganic Chemistry, Indian Association for the Cultivation of Science. Financial support received from the Council of Scientific and Industrial Research, New Delhi, India, is also acknowledged.

References

1 (*a*) P. Basu, S. Pal, and A. Chakravorty, *J. Chem. Soc., Chem. Commun.*, 1989, 977; (*b*) P. Basu, S. Bhanja Choudhury, S. Pal, and A. Chakravorty, *Inorg. Chem.*, 1989, **28**, 2680; (*c*) D. Ray and A. Chakravorty, *ibid.*, 1988, **27**, 3292.
2 I. B. Benson, J. Hunt, S. A. R. Knox, and V. Oliphant, *J. Chem. Soc., Dalton Trans.*, 1978, 1240.
3 J. Powell, *J. Chem. Soc., Chem. Commun.*, 1989, 200.
4 (*a*) J. Hyde, K. Venkatasubramanian, and J. Zubieta, *Inorg. Chem.*, 1978, **17**, 414; (*b*) J. P. Fackler, jun., and W. J. Zegarski, *J. Am. Chem. Soc.*, 1973, **95**, 8566.

5 A. Pramanik, N. Bag, D. Ray, G. K. Lahiri, and A. Chakravorty, unpublished work.
6 (*a*) B. Bleaney and M. C. M. O'Brien, *Proc. Phys. Soc., London, Sect. B*, 1956, **69**, 1216; (*b*) J. S. Griffith, 'The Theory of Transitional Metal Ions,' Cambridge University Press, London, 1961, p. 364; (*c*) G. K. Lahiri, S. Bhattacharya, S. Goswami, and A. Chakravorty, *J. Chem. Soc., Dalton Trans.*, 1990, 561; (*d*) G. K. Lahiri, S. Bhattacharya, B. K. Ghosh, and A. Chakravorty, *Inorg. Chem.*, 1987, **26**, 4324; (*e*) G. K. Lahiri, S. Bhattacharya, M. Mukherjee, A. K. Mukherjee, and A. Chakravorty, *ibid.*, p. 3359.
7 C. Daul and A. Goursot, *Inorg. Chem.*, 1985, **24**, 3554; N. Bag, G. K. Lahiri, S. Bhattacharya, L. R. Falvello, and A. Chakravorty, *Inorg. Chem.*, 1988, **27**, 4396.
8 R. S. Nicholson and I. Shain, *Anal. Chem.*, 1964, **36**, 706.
9 N. Serpone and D. G. Bickley, *Prog. Inorg. Chem.*, 1972, **17**, 391 and refs. therein.
10 D. E. Richardson, D. D. Walker, J. E. Sulton, K. O. Hodgson, and H. Taube, *Inorg. Chem.*, 1979, **18**, 2216; M. E. Gress, C. Creutz, and C. O. Quicksall, *ibid.*, 1981, **20**, 1522; D. S. Eggleston, K. A. Goldsby, D. J. Hodgson, and T. J. Meyer, *ibid.*, 1985, **24**, 4573; J. F. Wishart, A. Bino, and H. Taube, *ibid.*, 1986, **25**, 3318.
11 N. Bag, G. K. Lahiri, and A. Chakravorty, *J. Chem. Soc., Dalton Trans.*, 1990, 1557.
12 A. M. Bond, B. S. Grabaric, and Z. Grabaric, *Inorg. Chem.*, 1978, **17**, 1013; A. M. Bond, S. W. Carr, and R. Colton, *ibid.*, 1984, **23**, 2343; A. M. Bond, T. W. Hambley, D. R. Mann, and M. R. Snow, *ibid.*, 1987, **26**, 2257 and refs. therein.
13 R. D. Rieke, H. Kojima, and K. Öfele, *J. Am. Chem. Soc.*, 1976, **98**, 6735; C. M. Elson, *Inorg. Chem.*, 1976, **15**, 469; A. Vallat, M. Person, L. Roullier, and E. Laviron, *ibid.*, 1987, **26**, 332; M. M. Bernardo, P. V. Robandt, R. R. Schroeder, and D. B. Rorabacher, *J. Am. Chem. Soc.*, 1989, **111**, 1224.
14 B. E. Bursten, *J. Am. Chem. Soc.*, 1982, **104**, 1299; D. M. P. Mingos, *J. Organomet. Chem.*, 1979, **179**, C29.
15 B. P. Sullivan and T. J. Meyer, *Inorg. Chem.*, 1982, **21**, 1037.
16 A. R. Chakravarty and A. Chakravorty, *Inorg. Chem.*, 1981, **20**, 275.
17 T. A. Stephenson and G. Wilkinson, *J. Inorg. Nucl. Chem.*, 1966, **28**, 945.
18 R. G. Wilkins, 'The Study of Kinetics and Mechanism of Reactions of Transition Metal Complexes,' Allyn and Bacon, Inc., Boston, 1974.
19 G. M. Sheldrick, 'SHELXTL-Plus 88, Structure Determination Softward Programs,' Nicolet Instrument Corporation, Madison, 1988.
20 C. K. Johnson, ORTEP, Report ORNL-3794, Oak Ridge National Laboratory, Tennessee, 1965.

Received 18*th June* 1990; *Paper* 0/02737E